Article scientifique   Article   2021   Published version   Open Access

- -

The DEAD-box RNA helicase RhlE2 is a global regulator of Pseudomonas aeruginosa lifestyle and pathogenesis

- -

Hausmann, Stéphane; Gonzalez, Diego; Geiser, Johan; Valentini, Martina

The DEAD-box RNA helicase RhlE2 is a global regulator of *Pseudomonas aeruginosa* lifestyle and pathogenesis

Stéphane Hausmann[1],[†], Diego Gonzalez[2],[†], Johan Geiser[1] and Martina Valentini ⓘ [1],*

[1]Department of Microbiology and Molecular Medicine, CMU, Faculty of Medicine, University of Geneva, Geneva, Switzerland and [2]Laboratory of Microbiology, Institute of Biology, Faculty of Sciences, University of Neuchâtel, Neuchâtel, Switzerland

ABSTRACT

RNA helicases perform essential housekeeping and regulatory functions in all domains of life by binding and unwinding RNA molecules. The bacterial RhlE-like DEAD-box RNA helicases are among the least well studied of these enzymes. They are widespread especially among Proteobacteria, whose genomes often encode multiple homologs. The significance of the expansion and diversification of RhlE-like proteins for bacterial fitness has not yet been established. Here, we study the two RhlE homologs present in the opportunistic pathogen *Pseudomonas aeruginosa*. We show that, in the course of evolution, RhlE1 and RhlE2 have diverged in their biological functions, molecular partners and RNA-dependent enzymatic activities. Whereas RhlE1 is mainly needed for growth in the cold, RhlE2 also acts as global post-transcriptional regulator, affecting the level of hundreds of cellular transcripts indispensable for both environmental adaptation and virulence. The global impact of RhlE2 is mediated by its unique C-terminal extension, which supports the RNA unwinding activity of the N-terminal domain as well as an RNA-dependent interaction with the RNase E endonuclease and the cellular RNA degradation machinery. Overall, our work reveals how the functional and molecular divergence between two homologous RNA helicases can contribute to bacterial fitness and pathogenesis.

GRAPHICAL ABSTRACT
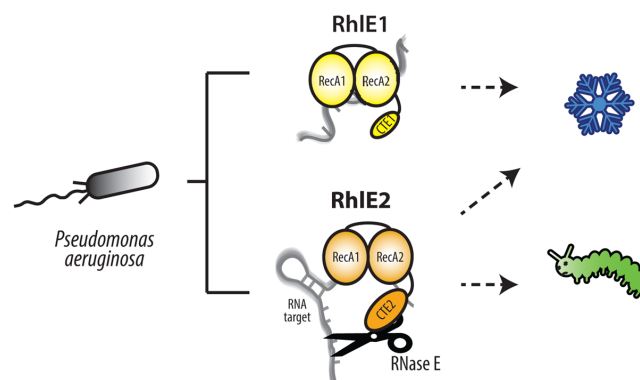
INTRODUCTION

DEAD-box RNA helicases are ATP-hydrolysing enzymes that remodel RNA structure and RNA–protein complexes (1). DEAD-box RNA helicases are found in all three domains of life, as well as in some viruses. They are identified on the basis of highly conserved amino acid motifs within their catalytic core, 'DEAD' being one of those motifs (2,3). The enzymatic core is flanked by variable N- and C-terminal extensions, that can regulate the core catalytic activity or coordinate interactions with RNA molecules or proteins (4–7). The *Escherichia coli* DbpA RNA helicase, for example, has an RNA-binding domain (RBD) at its C-terminus, which binds to hairpin 92 of 23S ribosomal RNA specifically (8). From bacteria to humans, DEAD-box RNA helicases are needed to maintaining basal RNA metabolism, by controlling mRNA translation, RNA degradation, and ribosome biogenesis (1). In bacteria, DEAD-box RNA helicases can also regulate environmental adaptation, host colonization and, in the case of pathogens, infectious processes (9–11).

Bacterial DEAD-box RNA helicases can be classified into three major phylogenetic groups: DbpA-like RBD-

containing proteins, RBD-lacking proteins, and RhlE-like proteins [12]. The RhlE-like RNA helicases, named after the *Escherichia coli* homolog, seem to have originated from the duplication, in a Proteobacterial ancestor, of RBD-lacking enzyme; they have then expanded and can be present in several homologs per genome [12]. The function of RhlE-like proteins seems to vary across species and their mechanism of action is not understood. No phenotype linked to *rhlE* deletion has been described in *E. coli*, *Pseudomonas syringae* LZ4W, and *Mycobacterium tuberculosis*, while deletion of *rhlE* affects cold acclimation in *Yersinia pseudotuberculosis* and *Caulobacter crescentus* [13–18]. In *E. coli*, RhlE interacts with the SrmB and CsdA RNA helicases during ribosome biogenesis, although the exact regulatory mechanism is not yet deciphered; in vitro *E. coli* RhlE also binds to the RNase E endonuclease and helps with RNA degradation, even if the conditions in which the interaction occurs in vivo are unknown [19,20]. In *P. syringae* LZ4W, *M. tuberculosis,* and *C. crescentus*, RhlE is described as a core component of the RNA degradosome machinery [13,17,18].

In the present study, we investigate the role of RhlE proteins in the Gram-negative bacterium *Pseudomonas aeruginosa*. This bacterium is widespread across multiple ecological niches, including a variety of hosts ranging from insects to mammals [21–23]. In humans, *P. aeruginosa* infections are life-threatening for immunocompromised and immunodeficient people, intensive care patients, patients with cystic fibrosis, or other chronic obstructive pulmonary diseases [24–28]. As an opportunistic pathogen, *P. aeruginosa* possesses a remarkable virulence plasticity, being able to colonize different type of organs and modify its virulence strategy and physiology in response to the context [29]. Our knowledge on DEAD-box RNA helicases and their role in *P. aeruginosa* is scarce at best [30].

We noticed that the genome of *P. aeruginosa* encodes two *rhlE* genes, PA3950 (*rhlE1*) and PA0428 (*rhlE2*), making the bacterium an ideal model to study proteobacterial RhlE function. Here, we reveal that both RhlE1 and RhlE2 are important for *P. aeruginosa* cold adaptation. In addition, *rhlE2* mutation results in a broad effect on motility, biofilm formation, and virulence, which makes it a global regulator. We assess RhlE1 and RhlE2 RNA preferences in vitro and identify the RhlE2 regulon in vivo. Moreover, we define a model of RhlE2 mechanism of action whereby RhlE2 affects RNA stability through an unusual interaction with RNase E, which is dependent on both RNA and RhlE2 unique C-terminal extension. Finally, we discuss the phylogenetic diversity of RhlE proteins by comparing *P. aeruginosa* RhlE homologs with the previously characterized RhlE proteins in other Proteobacteria.

MATERIALS AND METHODS

Bacterial strains and culture conditions

Bacterial strains and plasmids used in this study are listed in Supplementary Table S1. Cells were grown in Luria Broth (LB) or nutrient yeast broth (NYB) [31,32] medium, with shaking at 180 rpm and at 37°C. Nutrient agar (NA) was used as a solid medium. When required, antibiotics were added to these media at the following concentrations: 100 μg/ml ampicillin, 25 μg/ml tetracycline and 10 μg/ml gentamicin for *E. coli*; and 50 μg/ml gentamicin and 50 μg/ml tetracycline for *P. aeruginosa*.

Genetic techniques

DNA cloning and plasmid preparation were performed according to standard methods [33]. Oligonucleotides used for cloning procedures are listed in Supplementary Table S2. Restriction and DNA-modifying enzymes were used following the instructions of the manufacturers. Transformation of *E. coli* DH5α, *E. coli* TOP10 (for cloning) and *P. aeruginosa* was carried out by heat-shock and electroporation, respectively [34]. The construction of engineered plasmids and strains is detailed in Supplementary Information. All plasmids and strains were verified by PCR and sequencing.

ATPase reaction

Reaction mixtures (15 μl) containing 50 mM Tris–HCl, pH 8.0, 5 mM DTT, 2 mM MgCl$_2$, 1 mM ATP, RNA as specified, and enzyme as specified were incubated for 15 min at 37°C. The reactions were quenched by adding 3.8 μl of 5 M formic acid. Aliquots (2 μl) were applied to a polyethylenimine(PEI)-cellulose thin layer chromatography (TLC) plates (Merck), which were developed with 1 M formic acid, 0.5 M LiCl. ^{32}Pi release was quantitated by scanning the chromatogram with laser Scanner Typhoon FLA 7000 (General Electric). Oligo(ribo)nucleotides used (purchased from Microsynth) are listed in Supplementary Table S3.

Total RNA extraction

PAO1 wild type, PAO1Δ*rhlE1*, PAO1Δ*rhlE2* and PAO1Δ*rhlE1*Δ*rhlE2* mutants were grown at 37°C in swarming condition or on NYB until OD ∼1.5 with vigorous shaking. Cells were harvested using the RNA bacteria protect solution (QIAGEN). Total RNAs was extracted and purified using Monarch RNA isolation kit (NEB), treated with DNase I (Promega) three times to remove contaminating genomic DNA and re-purified again using phenol–chloroform. Eventual DNA contamination was tested by PCR with 40 cycles and different couples of primers (Supplementary Table S4) and RNA integrity was controlled by agarose gel electrophoresis.

RNA sequencing

PAO1 wild type, PAO1Δ*rhlE1*, PAO1Δ*rhlE2* and PAO1Δ*rhlE1*Δ*rhlE2* mutants were grown in 12-cm square swarming plates. After O/N incubation at 37°C, samples from six plates were pooled and total RNA was isolated from as described above. Two replicates of either strain were therefore obtained. Ribosomal RNA was depleted with Ribo-Zero rRNA Removal Kit (Illumina). Then, libraries were prepared using the Illumina TruSeq

stranded mRNA kit and validated on the Bioanalyzer 2100 (Agilent). Samples were sequenced using the Illumina HiSeq 2000, 100 bp single end read at the iGE3 genomics platform of the University of Geneva. After removal of the adaptors, the sequences were quality trimmed and filtered with *fastp* 0.20.0 using default parameters (35). The resulting reads were then mapped onto the PAO1 reference genome (NC_002516.2) using *bowtie2* 2.3.4.3 (36). Reads mapping on defined features were counted using *HTSeq* 0.11.1 (37). Analysis was carried out in R 3.6.3 (38) using *edgeR* 3.30.0 (39) after filtering for genes with genes with less than 4 reads in two samples or more. Statistical analysis of differential expression between the four strains was done using the robust quasi-likelihood method provided in EdgeR package (glmQLFit function). KEGG analysis was carried out using *limma*'s *kegga* function (40). All RNAs with a log2-fold change greater than 1 and a multiple testing adjusted *P*-value below 0.05 were considered differentially expressed. Raw files and read counts per gene have been deposited in the NCBI Gene Expression Omnibus (GEO) database under the accession number GSE166986.

RNA decay analysis

For decay analysis, rifampicin to 250 µg/ml was added to PAO1 wild type, PAO1Δ*rhlE2* liquid culture grown to OD600 of ∼1.5 and aliquots were withdrawn at the indicated times. RNA was extracted and used for RT-qPCR analysis using primers listed in Supplementary Table S4.

Pull-down assays

PAO1Δ*rhlE1*::P$_{BAD}$-3xFLAG_RhlE1, PAO1Δ*rhlE2*::P$_{BAD}$_RhlE2, PAO1Δ*rhlE2*::P$_{BAD}$-3xFLAG_RhlE2 and PAO1Δ*rhlE2*::P$_{BAD}$-3xFLAG_RhlE2$_{1-434}$ cultures were grown in 2 l flasks with 400 ml NYB plus 0.05% arabinose to an O.D ∼1.8–2.0, then pelleted by centrifugation and stored at –80°C for at least 12 h. Pellets were re-suspended in ice-cold IP buffer (20 mM HEPES pH 7.4, 300 mM NaCl, 1 mM EDTA, protease inhibitor) and cells were lysed by sonication. Samples were then centrifuged (15 000 g, 60 min, 4°C), the supernatant (soluble fraction) was collected and 1.0% (v/v) Triton X-100 was added and incubated at 4°C with end-over-end agitation for 20 min. Then, samples were incubated for 4 h with 20 µg/ml ANTI-FLAG M2 affinity gel (Sigma) (4°C, end-over-end agitation). Samples were pelleted by centrifugation (3000 g, 1 min 4°C), the supernatant was discarded, and the beads re-suspended in 1.0 ml ice-cold IP buffer. This wash step was repeated 5 times. Elution was performed twice in 100 µl 3xFLAG peptide (Sigma) at final concentration of 100 µg/ml. The presence of FLAG-tagged RhlE proteins was confirmed by immunoblotting, and co-eluting proteins were detected by Orbitrap mass spectrometry or by SDS-page followed by protein band extraction and identification by mass spectrometry. For RNase A treatment experiment, half of each sample was treated with 0.06 µg/µl RNase A and incubated for 40 minutes on ice before the affinity purification on ANTI-FLAG beads.

Phylogenetic analysis

RhlE homologs were identified from previously published analyses (9,12). Amino acid sequences retrieved from the NCBI RefSeq database (41) and aligned with MUSCLE (42). Sequences of RecQ (PA3344) were added as outgroup. The 790 sequences, together with *P. aeruginosa* RecQ (PA3344), were clustered into 148 groups using *cd-hit* (43) with a 0.9 identity threshold. The representative sequences of the clusters were aligned with *muscle* 3.8.31 (42) and truncated from their variable CTE; the alignment was then refined using the same software. A tree was produced from the alignment using *fasttree* 2.1.10 (44) with the -gamma option and Whelan-And-Goldman 2001 model of amino acid evolution; branches were collapsed below a support value of 0.6 using *TreeGraph* 2.15 (45). The final tree figure was produced thanks to *FigTree* 1.4.4 (Rambaut, 2019).

Other methods

Phenotypic assays, RhlE1 and RhlE2 purifications, β-Galactosidase assays, bacterial two-hybrid assay, virulence factor production assays, in vivo virulence assays, real-time quantitative PCR (RT-qPCR), electrophoretic mobility shift assays and helicase assays are detailed in Supplementary Information.

RESULTS

Pseudomonas aeruginosa encodes two RhlE-like RNA helicases with different origin and characteristics

The RhlE-like group of RNA helicases is widespread in Proteobacteria, with sometimes several homologs present in a single genome (9,12). The genome of *P. aeruginosa* PAO1, like that of most *Pseudomonas* species, encodes two RhlE-like proteins, RhlE1 (PA3950) and RhlE2 (PA0428), that belong to two distinct terminal branches of the RhlE phylogenetic tree (Figure 1A and Supplementary Figure S1). RhlE1 is found on a branch represented mostly in environmental bacteria, including *Vibrio, Shewanella*, *Legionella* and *Azotobacter* species, while RhlE2 belongs to a clade which includes mostly *Pseudomonas* species (Supplementary Figure S1). RhlE1 and RhlE2 are 51% and 43% identical to *E. coli* RhlE, respectively (Figure 1B). The canonical RecA1 and RecA2 domains, characteristic of helicases, and the ten short motifs typical of DEAD-box RNA helicases, are conserved in all RhlE-like proteins (Supplementary Figure S2). However, the C-terminal extension (CTE) presents high diversity and does not show any global pattern; it is therefore likely that RhlE CTEs are clade-specific and fast evolving. In particular, RhlE1 possesses a short CTE that contains a stretch of lysine-rich amino acids; RhlE2, on the other hand, possesses the longest CTE among RhlE-like proteins and includes a stretch of ∼50 amino acids rich in glycine and glutamate (Supplementary Figure S3).

Based on our bioinformatic analysis, we hypothesized that RhlE1 and RhlE2 might have distinct functions in *P. aeruginosa*. In order to test this hypothesis experimentally, we constructed strains deleted for *rhlE1* and *rhlE2* as well as
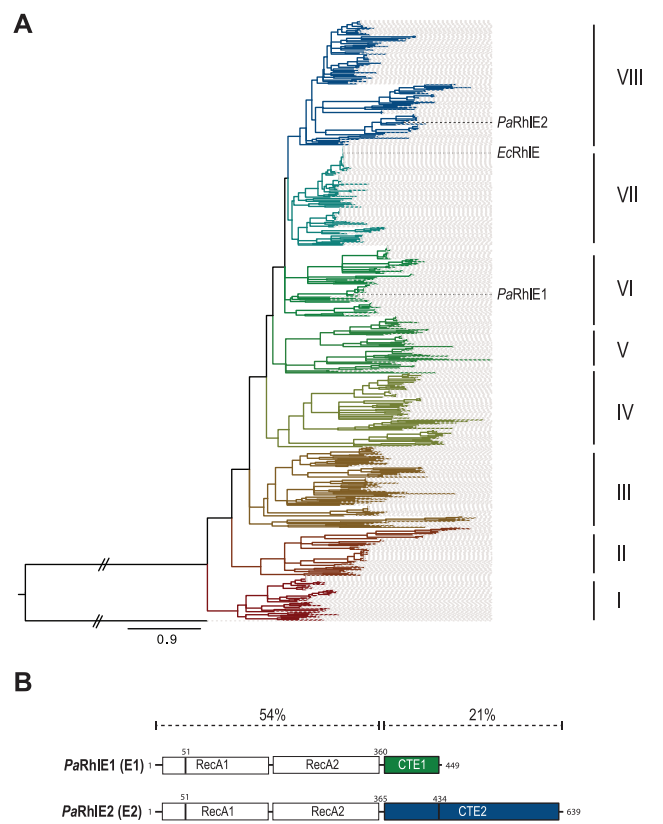
Figure 1. Phylogenetic tree of the bacterial RhlE DEAD-box proteins. (**A**) The tree is based on 148 representative sequences of bacterial DEAD-box helicases. The *P. aeruginosa* RecQ protein (PA3344) was used to root the tree. At least eight distinct groups can readily be identified; they are numbered I to VIII. (**B**) Linear representation of *P. aeruginosa* (Pa) RhlE1 (E1, PA3950) and RhlE2 (E2, PA0428) with the RecA1 and RecA2 domains in white boxes and their C-terminal extension (CTE) in green and blue boxes, respectively. The sequence identity with *E. coli* RhlE protein are indicated above. Vertical lines show the position of the mutation and truncation in RhlE1 and RhlE2 variants K51A and 1–434.
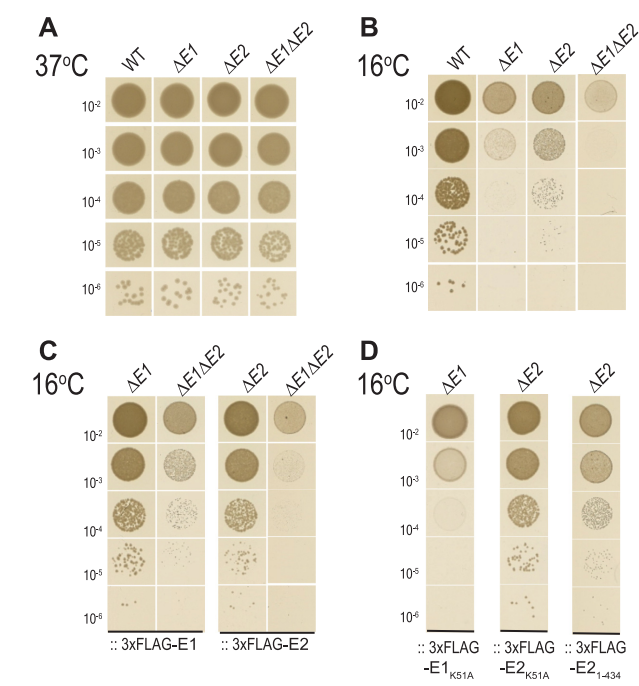

Figure 2. Role of RhlE1 and RhlE2 in *P. aeruginosa* cold adaptation. (**A**) 37°C and (**B**) cold (16°C) survival assays of wild type PAO1, Δ*rhlE1* mutant (ΔE1), Δ*rhlE2* mutant (ΔE2) and Δ*rhlE1*Δ*rhlE2* mutant (ΔE1ΔE2). (**C**) Complementation of cold sensitivity using mini-Tn7 constructs expressing 3xFLAG-tagged RhlE1 (::3xFLAG-E1), 3xFLAG-tagged RhlE2 (::3xFLAG-E2), (**D**), 3xFLAG-tagged RhlE1$_{K51A}$ (::3xFLAG-E1$_{K51A}$), 3xFLAG-tagged RhlE2$_{1-434}$ (::3xFLAG-E2$_{1-434}$) and 3xFLAG-tagged RhlE2$_{K51A}$ (::3xFLAG-E2$_{K51A}$). Strains background is indicated, and experimental details are described in Materials and Methods. At least three independent biological replicates were tested, results from a representative plate is shown.

the double mutant (Δ*rhlE1*Δ*rhlE2*) and studied their phenotypes.

RhlE1 and RhlE2 are both necessary for *P. aeruginosa* cold adaptation, but are not redundant

Since cold sensitivity is a common phenotype of strains lacking specific RNA helicases, including some RhlE-like helicases (9,13,14), we first tested the growth of the three mutant strains at different temperatures. Specifically, we spotted serial dilutions of liquid bacterial cultures on LB agar medium and incubating plates at 37 and 16°C. When observing growth on plate, two parameters were considered: colony forming units (CFUs) and colony size. At 37°C, the wild type, the single *rhlE1* or *rhlE2* deleted strains as well as the double Δ*rhlE1*Δ*rhlE2* mutant strain displayed similar growth (Figure 2A); the same was true in liquid cultures (Supplementary Figure S4). By contrast, at 16°C, deletion of *rhlE1* or *rhlE2* resulted in a growth defect (i.e., less CFUs and smaller colonies), which was further enhanced in the Δ*rhlE1*Δ*rhlE2* mutant (Figure 2B). Both RhlE1 and RhlE2 are therefore important for cold adaptation. However, the

same experiments also showed that the two proteins are not entirely redundant. While the loss of *rhlE1* produced a severe growth delay, the loss of *rhlE2* was only slightly deleterious. To further test the extent of functional overlap between the two proteins, we performed complementation experiments. We used a mini-Tn7 system to insert into the chromosomal Tn7 attachment site of Δ*rhlE1*, Δ*rhlE2* or Δ*rhlE1*Δ*rhlE2* mutants a copy of the *rhlE1* or *rhlE2* gene under the control of an arabinose-inducible promoter. As the genes carried by the mini-Tn7 constructs were cloned with a N-terminal 3xFLAG epitope, we could verify that the expression levels of the two constructs were comparable by immunoblot (Supplementary Figure S5). Growth of the *rhlE1* mutant at 16°C could be restored to wild type levels by the insertion of the mini-Tn7_3xFLAG-RhlE1 (::3xFLAG-E1) construct (Figure 2C); likewise, the *rhlE2* mutant could be complemented by the mini-Tn7_3xFLAG-RhlE2 (::3xFLAG-E2). However, we could not fully restore the growth at 16°C of the Δ*rhlE1*Δ*rhlE2* mutant by reintroducing any one of the *rhlE* genes (Figure 2C), nor complement the phenotype of one *rhlE* mutant with the other *rhlE* homolog (Supplementary Figure S6). Since they do not cross-complement each other during growth in the cold, RhlE1 and RhlE2 present some degree of functional specialization.

RhlE2 is a global lifestyle regulator in *P. aeruginosa*

Besides cold resistance, some bacterial RNA helicases have been shown to be involved in environmental adaptation or even pathogenicity via posttranscriptional gene regulation processes (9,11). We therefore tested whether RhlE1 and RhlE2 had an impact on medically relevant physiology and behaviour in *P. aeruginosa*. We first assessed the capacity of the *rhlE* mutant strains to move in liquid and on surfaces (Figure 3A) and to form biofilms (Figure 3B). All the experiments were carried at 37°C since the mutant strains did not present any growth defect at this temperature. Interestingly, the Δ*rhlE2* mutant was strongly affected in both motility (20, 2.5- and 15-fold reduction of swimming, twitching and swarming, respectively) and biofilm formation (3- and 1.5-fold decrease of early and mature biofilm, respectively) when compared to the wild type strain. Restoration of the Δ*rhlE2* mutant phenotypes to wild type level was observed by insertion of the mini-Tn7_3xFLAG-RhlE2 (Supplementary Figure S7). By contrast, deletion of *rhlE1* did not result in any significant phenotype; in accordance with this, the phenotype of the Δ*rhlE1*Δ*rhlE2* mutant did not differ from that of the Δ*rhlE2*. Furthermore, while complementation of the Δ*rhlE1*Δ*rhlE2* mutant with 3xFLAG-E2 was able to fully restore swarming motility to wild type levels, the Tn7 construct carrying *rhlE1* failed to do so (Figure 3C). Finally, the lack of a phenotype linked to a *rhlE1* deletion even in absence of *rhlE2* indicates that functional interaction among these two RNA helicases is limited (Figure 3A and B). Altogether, these results further support the functional divergence of the two RhlE homologs in *P. aeruginosa*. While RhlE1 has a specific role during cold adaptation, RhlE2 is involved in key cellular and behavioural processes and could therefore be considered a global lifestyle regulator.

RNA sequencing analysis reveals the importance of RhlE2 for *P. aeruginosa* virulence

To further define the function of RhlE homologs in *P. aeruginosa*, we characterized the transcriptome of all three *rhlE* mutant strains by RNA-sequencing. Because of its anticipated role as a global regulator, we decided to focus our investigation on RhlE2 and chose an experimental condition accordingly. The strongest phenotype of the Δ*rhlE2* mutant was seen under swarming conditions (Figure 4A). Swarming motility is a coordinated movement of a bacterial population on semi-solid surfaces (0.5–0.7% agar), which is mediated by flagella and surfactants (46). Importantly, the swarming behaviour is highly relevant to *P. aeruginosa* pathogenicity as it correlates with expression of virulence factors needed for epithelial surface colonization and lung infection through biofilm formation (47,48). The deletion of *rhlE2* affected about 15% of the transcriptome (*N* = 836 genes, *P*-value < 0.05, FC > 2) with 4% (N = 228) of the transcripts up-regulated and 11% (*N* = 608) down-regulated (Figure 4B, Supplementary Table S5). Differentially regulated genes were grouped into the corresponding KEGG pathways: genes involved in ribosome and secondary metabolite biosynthesis were enriched among the downregulated transcripts, while genes implicated in xenobiotic biodegradation and metabolism
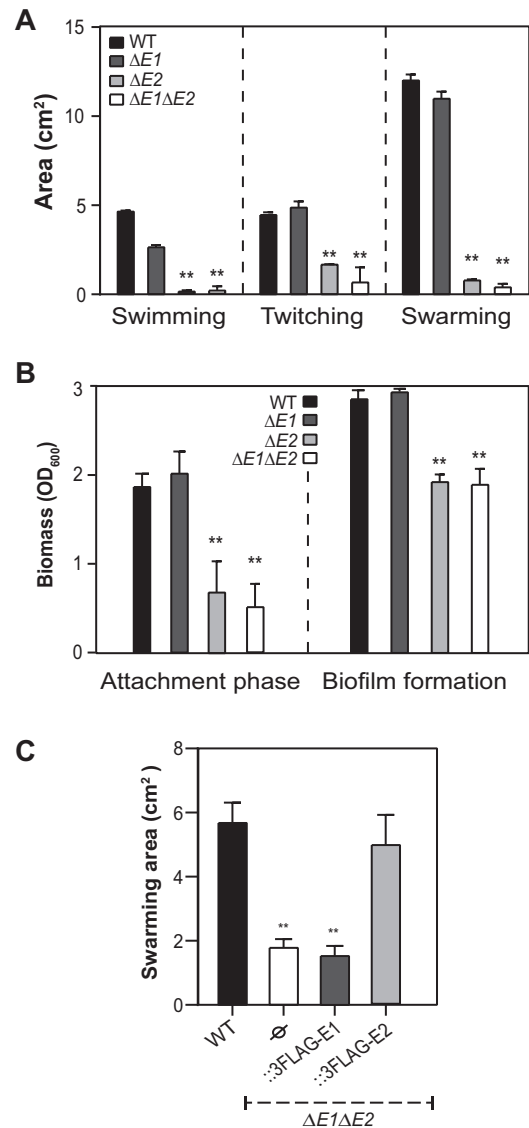

Figure 3. Role of RhlE1 and RhlE2 in *P. aeruginosa* motilities and biofilm formation. (**A**) Surface area covered by the swimming, swarming and twitching wild type PAO1 (WT, black diamonds), the Δ*rhlE1* mutant (ΔE1,dark grey triangles), the Δ*rhlE2* mutant (ΔE2, light grey circles) and the Δ*rhlE1*Δ*rhlE2* mutant (ΔE1ΔE2, white squares) cells (± standard deviation) as calculated by averaging data from four individual plates. (**B**) Surface attached biomass, measured by crystal violet staining, of wild type PAO1 and *rhlE1*/*rhlE2* mutant strains after 6 h (attachment phase) or 12 h (biofilm formation) of growth at 37°C in 24-μl plates. (**C**) Complementation of swarming motility using mini-Tn7 constructs carrying 3xFLAG-tagged RhlE1 (::3xFLAG-E1), 3xFLAG-tagged RhlE2 (::3xFLAG-E2) expressed in a Δ*rhlE1*Δ*rhlE2* mutant. Swarming assay in panel A uses minimal MMP medium supplemented with 20 mM glucose and 0.1% casamino acids, while in panel C swarming assays are performed in nutrient agar plates, optimizing the induction by arabinose (85) (see Supplemental information). Each value is the average of three different cultures ± standard deviation (*P < 0.05; **P < 0.01).

(e.g. 4-fluorobenzoate, chlorocyclohexane and chlorobenzene degradation) were overrepresented among upregulated ones (Supplementary Table S6). Consistent with the phenotypic analysis, *rhlE1* deletion had no significant impact on the cellular transcript levels neither in the wild type nor in
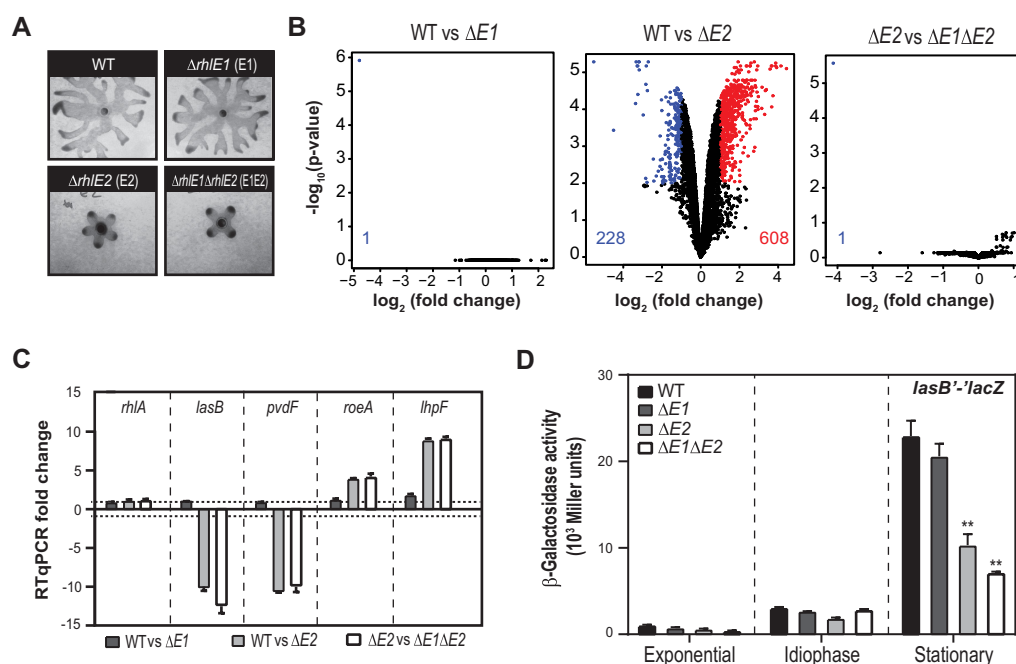
Figure 4. The RhlE2 regulon. (**A**) Example of wild type PAO1, Δ*rhlE1* mutant, Δ*rhlE2* mutant and the Δ*rhlE1*Δ*rhlE2* mutant swarming cells that were subjected to RNA-sequencing analysis. (**B**) Volcano plot representation of transcriptome comparison between the wild type PAO1 (WT) and Δ*rhlE1* (Δ*E1*) or Δ*rhlE2* (Δ*E2*) or Δ*rhlE1*Δ*rhlE2* (Δ*E1*Δ*E2*). Transcriptome analysis was performed in duplicate and for every duplicate, cells from six independent swarming colonies were pooled together. The genes are colored if they pass the thresholds for −log10 *P* value (*P* value < 0.05) and log fold change |FC| ≥2 (red, down-regulated in the Δ*E2*; blue, upregulated). (**C**) Relative transcript abundance in the wild type PAO1 and *rhlE1/rhlE2* mutant strains as determined by RT-qPCR (RT-qPCR fold change). Values are represented as averages of three independent replicates for every strain. (**D**) Cell density-dependent β-galactosidase expression of a transcriptional/translational *lasB'-'lacZ* fusion carried by plasmid pTS400 (54) in wild type PAO1 (black bars), Δ*rhlE1* mutant (Δ*E1*, dark grey bars), Δ*rhlE2* mutant (Δ*E2*, light grey bars) and Δ*rhlE1*Δ*rhlE2* mutant (Δ*E1*Δ*E2*, white bars). Each value is the average of three different cultures ± standard deviation (******P < 0.01).

the *rhlE2* mutant background at 37°C (Figure 4B). To validate the transcriptome analysis, we chose a set of putative RhlE2 targets and examined their abundance by RT-qPCR in the Δ*rhlE1*, Δ*rhlE2* and Δ*rhlE1*Δ*rhlE2* mutants as compared to the wild type strain under the conditions similar to the ones where the RNA-sequencing was performed. The chosen genes have been previously shown to either regulate swarming or being differentially regulated in this condition, such as *roeA*, coding for a diguanylate cyclase (49), *lhpF*, coding for the metabolic enzyme D-hydroxyproline dehydrogenase (50), the *lasB* elastase (51) and the *pvdF* pyoverdine synthase (52) encoding genes; the *rhlA* gene (encoding the chain A of the rhamnosyltransferase) was chosen as a negative control since it was unaffected by *rhlE2* mutation, but known to be necessary for swarming motility (53). In agreement with the RNA-seq data, *lasB* and *pvdF* mRNA levels were, respectively, 10.25 and 10.41-fold down-regulated in the Δ*rhlE2* mutant when compared to the wild type; while *roeA* and *lhpF* were, respectively, 3.98 and 8.94-fold up-regulated; *rhlA* mRNA levels were unchanged (Figure 4C). To further validate the observation concerning regulation of *lasB* expression, a transcriptional/translational *lasB'-'lacZ* fusion (54) was assayed for β-galactosidase activity in the four strains, at different growth phases in NYB (Figure 4D). Expression of *lasB* is dependent on cell-density and therefore maximal in stationary phase (55); the same trend was observed in all the mutants but in the Δ*rhlE2* and Δ*rhlE1*Δ*rhlE2* mutants the expression of the *lasB'-'lacZ* fu-

sion was reduced of ∼2.5-fold in stationary phase, when compared to the wild type and Δ*rhlE1* strains. This, again, confirms the validity of our transcriptome analysis.

Finally, we were able to confirm that some of the changes in gene expression resulted in actual differences in virulence factor levels. The extracellular levels of the LasB elastase, a secreted metalloendopeptidase inducing host cell/tissue injury (56), and pyocyanin, a redox-active molecule inducing oxidative stress in host cells (57), were assessed by spectrofluorometric-based assays. We found that the Δ*rhlE2* and Δ*rhlE1*Δ*rhlE2* mutants produced 2.6- and 3.6-fold less elastase and 2,1- and 2.4-fold less pyocyanin than the wild type, respectively, while the *rhlE1* deletion mutant did not exhibit any significant phenotypic difference compared to the wild type (Figure 5A and B).

RhlE2 affects *P. aeruginosa* virulence in *Galleria mellonella*

Based on our previous results, we conjectured that RhlE2 might be required to support *P. aeruginosa* pathogenesis *in vivo*. We used *Galleria mellonella* as a bacterial pathogenesis model (58) to test this hypothesis. In agreement with our predictions, the virulence of the Δ*rhlE2* and Δ*rhlE1*Δ*rhlE2* mutants proved to be significantly attenuated *in vivo*. Indeed, at 24 h post-infection the mortality of larvae injected with either Δ*rhlE2* or Δ*rhlE1*Δ*rhlE2* reached <40%, while the mortality rate of larvae challenged with wild type or Δ*rhlE1* strain was 80% (Figure 5C). Altogether, these re-
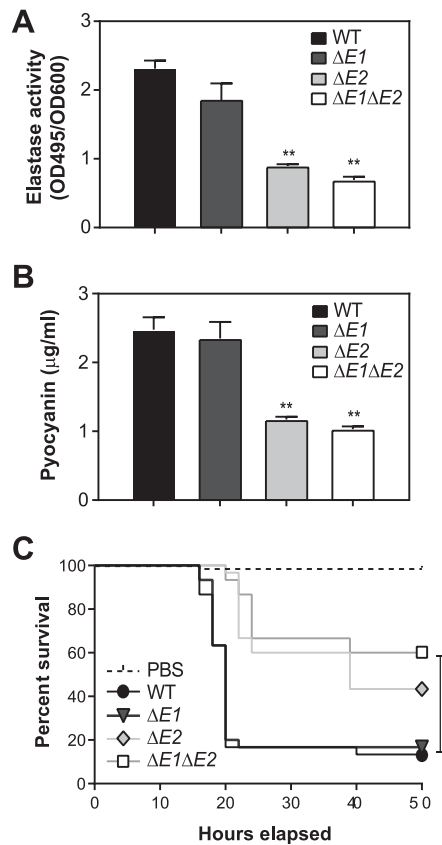
Figure 5. RhlE2 regulation of *P. aeruginosa* virulence. (**A**) Elastase activity and (**B**) pyocyanin levels of wild type PAO1 (black bars), Δ*rhlE1* mutant (ΔE1, dark grey bars), Δ*rhlE2* mutant (ΔE2, light grey bars) and Δ*rhlE1*Δ*rhlE2* mutant (ΔE1ΔE2, white bars) supernatant (**$P < 0.01$). (**C**) Survival curves of *G. mellonella* larvae infected with wild type PAO1 and *rhlE1*/*rhlE2* mutant strains. PBS, larvae injected with sterile physiological solution. (Survival analysis, Significance of the Wilcoxon's rank sum-test is displayed as ****$P < 0.0001$). Each experiment (A–C) was repeated at least with three different independent cultures for each strain, values indicated average from biological replicates ± standard deviation. For experimental details see Materials and Methods.

sults indicate that RhlE2 controls, directly and/or indirectly, the expression of virulence genes and is necessary for *P. aeruginosa* pathogenicity *in vivo*.

RhlE1 and RhlE2 display an RNA-dependent ATPase activity and an RNA unwinding activity in vitro

To explain the functional difference between RhlE1 and RhlE2, we aimed at characterizing their biochemical activity, starting with their RNA-dependent ATP-hydrolytic activity (2). We produced RhlE1 and RhlE2 in *E. coli* as N-terminal His_{10}-Smt3-tagged fusion and purified them from a soluble extract by adsorption to nickel-agarose and elution with 250 mM imidazole (Figure 6A). As control, we also purified the RhlE1 and RhlE2 catalytic mutants, in which the Lys51 of RhlE1 and RhlE2 within motif I (involved in ATP binding and hydrolysis) is replaced by an alanine, making the catalytic core inactive (59). As shown in Figure 6B, both recombinant RhlE1 and RhlE2 could catalyze the release of ^{32}Pi from [γ-^{32}P] ATP in the pres-

ence of poly(U) RNA (stretches of more than 150 ribonucleotides, heterogenous in size); the extent of ATP hydrolysis was proportional to the protein concentration. From the slope of the titration curves, we estimated that RhlE1 and RhlE2 hydrolyzed 0.0119 nmol and 0.0068 nmol ATP per ng of enzyme, respectively, during a 15 minutes reaction time. This translates into 758 mol of Pi formed per mol of RhlE1 and 597 mol of Pi formed per mol of RhlE2, and an estimated turnover number of 51 and 37 min^{-1}, respectively. These values indicate that both RhlE proteins have a similar ATPase activity in the presence of poly(U) RNA. As expected for DEAD-box RNA helicases, both RhlE1 and RhlE2 catalyzed no detectable ATP hydrolysis either in absence of RNA (Figure 6B) or when using poly(dT) DNA substrate (Supplementary Figure S8A). Moreover, the ATPase activity of RhlE1$_{K51A}$ and RhlE2$_{K51A}$ mutants were less than 1% of the activity of the respective wild type enzyme stimulated by poly(U) RNA (Figure 6C), validating that the observed RNA dependent phosphohydrolase activities of wild type RhlE1 and RhlE2 are intrinsic to the recombinant proteins. Like other RNA helicases, RhlE1 and RhlE2 exhibit an RNA-dependent phosphohydrolytic activity; this activity, however, is very similar in both enzymes and cannot be the basis of their functional divergence. We next focused on the RNA helicases ATP-dependent RNA unwinding activity (60). In *E. coli*, RhlE unwinds double-stranded RNA (dsRNA) in an ATP-dependent manner, irrespectively of the presence and location of single-stranded extensions (61). We observed similar properties for *P. aeruginosa* RhlE1 and RhlE2, although RhlE2 is significantly more efficient than RhlE1, which has a poor activity in the experimental conditions tested (Supplementary Figure S9A and B).

Characterization of the RhlE1 and RhlE2 RNA preferences

Despite having a similar ATPase activity in presence of poly(U), RhlE1 and RhlE2 ATPase activity could still differ depending on RNA molecule used as substrate. We examined the effect of RNA length on the ATPase activity of RhlE1 and RhlE2 by using a set of poly(U) RNA of defined lengths (U10, U16, U25 and U41, respectively). We found that the extent of phosphate release by RhlE1 with U41, U25, U16, U10 RNA substrate were 73, 27, 16, and 6% of the activity with poly(U) RNA, respectively, while the corresponding RhlE2 ATPase activity was 35, 12, 1 and <1% (Figure 6D). This result indicates that RhlE2 ATPase activity requires RNA oligomers of ≥25 nucleotides (nt), whereas RhlE1 can still be activated by RNA oligomers shorter than 16 nt.

We next examined whether the RNA secondary structure can affect the ATPase activity of RhlE proteins. To this purpose, we used three different 41-mer RNA substrates: a single-strand RNA (ssRNA), a stem loop of 8 bp with a 9-Us extension both at the 5′ and 3′ end (shRNA^{8bp}), and a blunt-ended stem-loop RNA molecule with 17 bp in the stem region (shRNA^{17bp}; see Supplementary Figure S10). RhlE1 had a similar activity with the three different RNA substrates, whereas the ATPase activity of RhlE2 was increased 3-fold with shRNA^{8bp} and 4-fold with a blunt-ended stem-loop RNA shRNA^{17bp}, compared to sin-
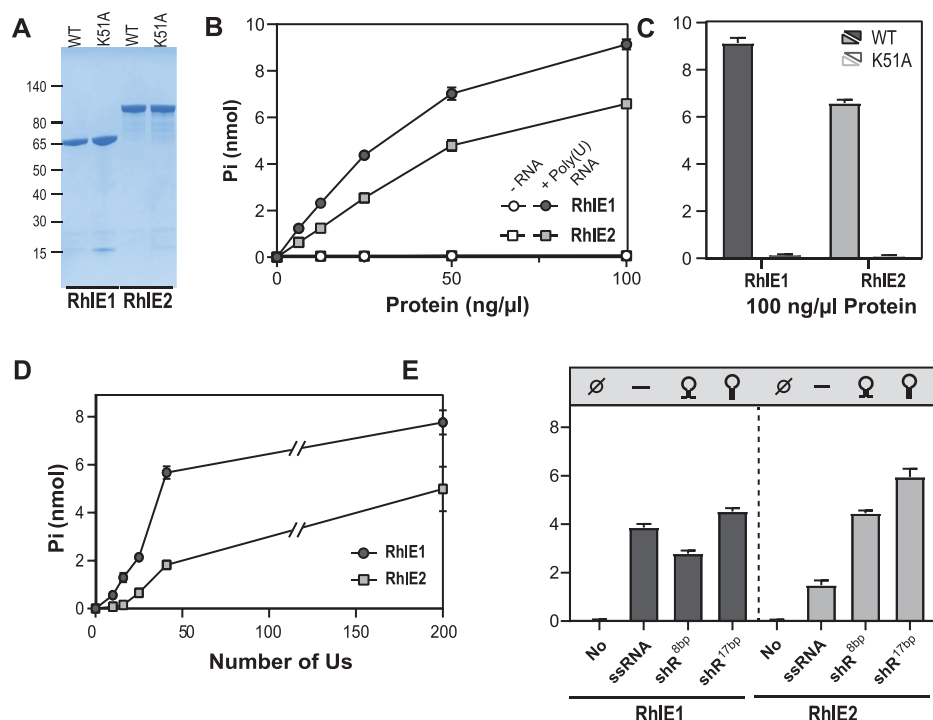
Figure 6. ATPase activity of recombinant RhlE1 and RhlE2. (**A**) RhlE proteins purification. Aliquots (2.5 μg) of the nickel-agarose preparations of wild type (WT) RhlE1(lane 1), and mutant K51A (lane 2), wild type (WT) RhlE2 (lane 3), and mutant K51A (lane 4) were analyzed by SDS-PAGE. The polypeptides were visualized by staining with Coomassie Blue dye. The positions and sizes (kDa) of marker polypeptides are indicated on the left. (**B**) RhlE proteins ATPase activity. Reaction mixtures (15 μl) containing 50 mM Tris–HCl (pH 8.0), 5 mM DTT, 2 mM $MgCl_2$, 1 mM [γ-^{32}P] ATP, 250 ng/μl Poly(U) (or no RNA; empty symbol), and enzyme as specified were incubated for 15 min at 37°C. Pi release was determined as described in Materials and Methods and was plotted as a function of input protein. (**C**) RhlE proteins catalytic mutants. Reaction mixtures (15 μl) containing 50 mM Tris–HCl (pH 8.0), 5 mM DTT, 2 mM $MgCl_2$, 1 mM [γ-^{32}P] ATP, 250 ng/μl Poly(U), and 100 ng/μl of enzyme as specified were incubated for 15 min at 37°C. The extends of ATP hydrolysis are plotted. (**D**) ATPase activity and RNA length. Reaction mixtures (15 μl) 50 mM Tris–HCl (pH 8.0), 5 mM DTT, 2 mM $MgCl_2$, 1 mM [γ-^{32}P] ATP, 2 μM polyribouridylic acid (either U41, U26, U16 or U10) as specified, and 50 ng/μl of RhlEs were incubated for 15 min at 37°C. The extends of ATP hydrolysis are plotted. (**E**) RNA hairpin recognition. Reaction mixtures (15 μl) 50 mM Tris–HCl (pH 8.0), 5 mM DTT, 2 mM $MgCl_2$, 1 mM [γ-^{32}P] ATP, 2 μM of an oligoribonucleotide as specified and 50 ng/μl of RhlEs were incubated for 15 min at 37°C. The extends of ATP hydrolysis are plotted. (B–E) Data are the average ± SEMs from three independent experiments.

gle strand RNA (ssRNA), indicating that RNA structure significantly affects the ATPase activity of RhlE2, but not that of RhlE1 (Figure 6E). Besides that, similar release of phosphate by RhlE1 and RhlE2 is observed with the two 41-mer U41 and ssRNA (5.7 nmol and 3.9 nmol Pi for RhlE1 and 1.8 and 1.5 nmol Pi for RhlE2, respectively), confirming that the ATPase activity of RhlE-like helicases display poor RNA sequence specificity (61–65). Of note, the 41-mer DNA substrates (shDNA, shDNA^{8bp} and shDNA^{17bp}) cannot activate RhlE1 and RhlE2 ATPase activity, confirming that RhlE1 and RhlE2 are strictly RNA dependent (Supplementary Figure S8B). Altogether, these results strongly suggest that the ATPase activity of RhlE1 and RhlE2 is stimulated differently depending on the length and structure of the RNA they bind to. It is worth mentioning that cleaving the N-terminal His$_{10}$-Smt3- tag does not affect the enzymatic activity of the proteins nor their RNA preference (Supplementary Figure S11).

Importance of RhlE1 and RhlE2 ATPase activity for their regulatory action in vivo

Having validated that the replacement of the lysine by alanine in the motif I abolished the ATPase activity of RhlE1

and RhlE2, we sought to determine if the observed catalytic activity of RhlE1 or RhlE2 was necessary for their role *in vivo*. We constructed mini-Tn7 variants expressing the 3xFLAG-RhlE1$_{K51A}$ or 3xFLAG-RhlE2$_{K51A}$ mutant and assessed their capacity to complement the phenotypes of the corresponding deleted strain. Expression of the RhlE1 catalytic mutant (3xFLAG-E1$_{K51A}$) was not able to restore the growth at 16°C of the *rhlE1* mutant, while, surprisingly, the RhlE2$_{K51A}$ construct (3xFLAG-E2$_{K51A}$) was able to sustain growth at 16°C of the Δ*rhlE2* mutant (Figure 2D). This suggests that RhlE2 ATPase activity is not essential for at least some of its functions. Since this result was quite unexpected, we confirmed, by resequencing, that the construct within the mini-Tn7 had not accumulated unwanted mutations and that the mutant phenotype suppression was dependent on arabinose induction. In agreement with this, we observed that the swarming motility of the Δ*rhlE2* mutant expressing 3xFLAG-E2$_{K51A}$ was similar to the Δ*rhlE2* mutant (Figure 7A). We also used the *lasB'-'lacZ* fusion as a proxy of RhlE2 regulatory activity, as it was downregulated in the Δ*rhlE2* mutant (Figure 4D). Again, the expression of the fusion was similarly affected in the Δ*rhlE2* mutant expressing RhlE2$_{K51A}$ as in the Δ*rhlE2* mutant, while the 3FLAGxRhlE2 construct was restoring the expression
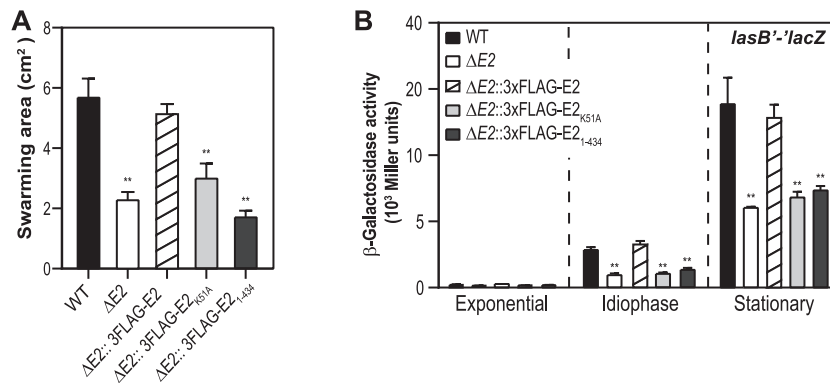
Figure 7. Complementation assays with RhlE2 variants. (**A**) Swarming motility and (**B**) *lasB'-'lacZ* expression of wild type PAO1, Δ*rhlE2* mutant (Δ*E2*) and Δ*rhlE2* mutant carrying a mini-Tn7 construct expressing either 3xFLAG-tagged RhlE2 (::3xFLAG-E2) or 3xFLAG-tagged RhlE2$_{1-434}$ (::3xFLAG-E2$_{1-434}$), or 3xFLAG-tagged RhlE2$_{K51A}$ (::3xFLAG-E2$_{K51A}$). Each experiment was repeated at least with three different independent cultures for each strain, values indicated average from biological replicates ± standard deviation (**P < 0.01). For experimental details, see Materials and Methods.

of *lasB'-'lacZ* in the Δ*rhlE2* mutant to the wild type levels (Figure 7B). In all these conditions, unlike at 16°C, the catalytic activity of RhlE2 is essential for its regulatory action. This indicates that, unlike RhlE1, RhlE2 performs its function through two semi-independent biochemical processes.

RhlE2 interacts with the Ribonuclease E via RNA

The differences in biochemical activity observed between RhlE1 and RhlE2 might not be the only explanation of their functional divergence. Their interaction with different protein partners could also determine their specificity. To test this hypothesis, we probed RhlE1 and RhlE2 interacting partners by protein affinity assays (pull-downs) using *P. aeruginosa* Δ*rhlE1*::3xFLAG-RhlE1 and the Δ*rhlE2*::3xFLAG-RhlE2 strains, respectively. Strains were grown at 37°C to an OD600 of ∼1.5 in presence of 0.02% of arabinose and the proteins were purified using an anti-FLAG antibody conjugated resin (see Material and Methods). The protein profile of the eluted fractions was first analysed by SDS page and then by mass-spectrometry (Figure 8A). As control, we used an Δ*rhlE2* strain expressing untagged RhlE2 (CN). Two bands appeared specifically in the elution profile of the 3xFLAG-RhlE2 construct, one at ∼80 kDa corresponding to 3xFLAG-RhlE2 and one additional band at ∼140 kDa. The latter was excised from the gel and identified by mass-spectrometry as RNase E, the core component of the bacterial RNA degradosome. By contrast, no band other than RhlE1 was visible in the elution of the 3xFLAG-RhlE1 pull-down (Figure 8B). To identify putative partners that were not visible as marked bands on denaturing gels, the entire eluted samples were further analysed by mass-spectrometry. Additional proteins were consistently enriched >2-fold in the 3xFLAG-RhlE2 elution of three independent pull-down experiments when compared to the negative control (Figure 8C). Interestingly, the three most enriched proteins in the 3xFLAG-RhlE2 sample were the ribonucleases RNase E, PNPase and RNase R, suggesting a role of RhlE2 in RNA processing and degradation. The fourth most enriched protein

was the DnaK chaperone, which appeared enriched in the 3xFLAG-RhlE1 sample as well.

Next, we asked whether the observed RhlE2-protein interactions were direct protein-protein interactions or indirect interactions mediated by RNA. To address this question, additional 3xFLAG-RhlE2 pull-downs were performed by pre-treating cell lysates with RNase A. The enrichment of peptides corresponding to RNase E, PNPase and RNase R was lost in the 3xFLAG-RhlE2 elution sample treated with RNase A, when compared to the untreated sample, reaching background levels comparable to the negative control; by contrast, peptides corresponding to DnaK were still present (Figure 8C). Thus, we conclude that RNA is necessary to mediate or stabilize any interaction of RhlE2 with RNases.

To confirm the pull-down results, we performed bacterial two-hybrid assays, which report on protein interactions based on proximity of split T25-T18 adenylyl cyclase domains (66). Co-expression of T25-*rhlE2* and T18-*rne*, *rne* encoding RNase E, restored the enzyme activity and resulted in red colonies when cells were grown in Congo Red medium and in a significant increase of β-galactosidase activity compared to controls (Figure 8D). In agreement with the pull-down assays, T25-RhlE1 interaction with T18-RNase E was not detected. In addition, the K51A mutation did not affect interaction of RhlE2 with T18-RNase E. Finally, interaction of RhlE2 with RNase R and PNPase was not detected via bacterial two-hybrid assays, indicating that these interactions probably occur indirectly via RNase E (Supplementary Figure S12).

The CTEs of RhlE2 is needed for interaction with RNase E and protein function *in vivo*

The CTE of a subset of RNA helicases is essential to their activity *in vivo* as it mediates interactions with other proteins and/or recognition of target RNAs (8,67,68). RhlE2 possesses a unique CTE that differs from the one found in RhlE1 and the other RhlE homologs investigated so far (Supplementary Figure S2). To assess the importance of RhlE2 CTE, we tried to complement the Δ*rhlE2* strain with a mini-Tn7 construct carrying 3xFLAG-RhlE2 truncated
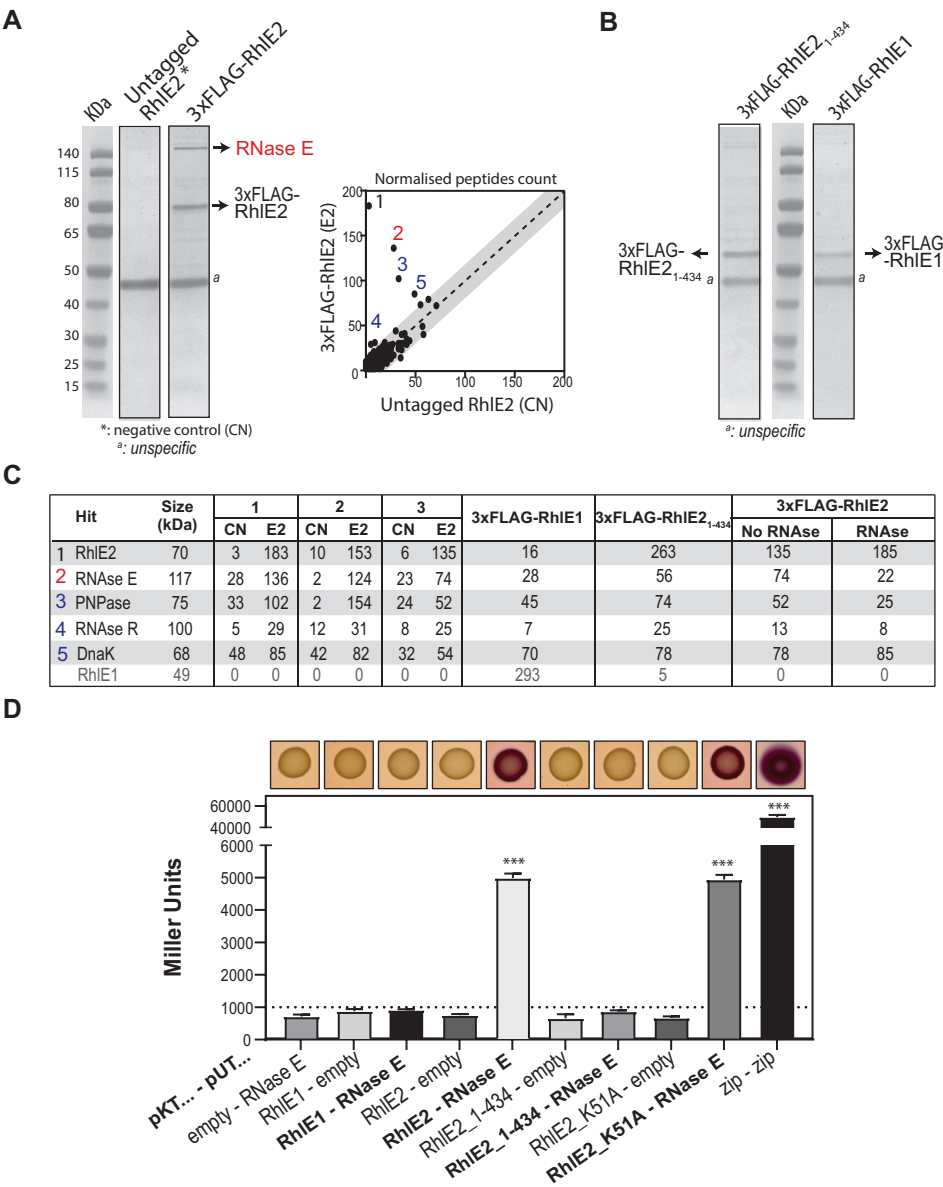
Figure 8. RhlE2 - RNase E interaction. Pull-down assays of 3xFLAG-RhlE2, 3xFLAG-tagged RhlE2$_{1-434}$ and 3xFLAG-RhlE1 and SDS-page analysis of co-eluting proteins. Culture of (**A**) $\Delta rhlE2$ mutant carrying a mini-Tn7 construct expressing either 3xFLAG-tagged RhlE2 (3xFLAG-RhlE2) or RhlE2 (untagged RhlE2) or of (**B**) $\Delta rhlE2$ mutant carrying a mini-Tn7 construct expressing 3xFLAG-tagged RhlE2$_{1-434}$ (3xFLAG-RhlE2$_{1-434}$) and $\Delta rhlE1$ mutant carrying a mini-Tn7 construct expressing 3xFLAG-tagged RhlE1 (3xFLAG-RhlE1) were grown on NYB with 0.05% arabinose at 37°C up to idiophase of growth (O.D. ~1.8). Arrowheads proteins were identified by mass-spectrometry. Other proteins co-eluting with 3xFLAG-RhlE2 were identified by mass-spectrometry of the eluted fraction and comparison with peptide counts present in the untagged RhlE2 sample is shown in panel A (right). (**C**) Quantification of top five proteins which peptides were significantly enriched in 3xFLAG-RhlE2, meaning RhlE2, RNase E, PNPase, RNase R and Dna K as compared to other strains (CN, negative control/untagged strain; 3xFLAG-RhlE1 and 3xFLAG-RhlE2$_{1-434}$). Pull-down of 3xFLAG-RhlE2 was performed in triplicates (1, 2 and 3), as well in absence (no RNase) and presence (RNase) of RNase A treatment. (**D**) Reconstitution of adenylate cyclase in the *E. coli* strain BTH101 using a bacterial two-hybrid approach was detected by red colour of colonies due to media acidification derived from maltose fermentation when colonies were grown on McConkey plates containing 1% maltose, 0.5 mM IPTG, 100 μg/ml ampicillin, and 50 μg/ml chloramphenicol agar plates, as shown. The interactions were also quantified in Miller Units by β-galactosidase assays using liquid cultures of the same strains. Each value is the average of three different cultures ± standard deviation (*$P < 0.05$; **$P < 0.01$).

of its C-terminal region (3xFLAG-RhlE2$_{1-434}$). RhlE2 without CTE (amino-acid 434–648) was not able to restore all tested phenotypes, *i.e.* growth at 16°C, swarming motility and expression of the *lasB'-'lacZ* reporter fusion at wild type levels (Figures 2D, 7 and Supplementary Figure S5).

We hypothesized that the RhlE2-RNase E interaction could be mediated by the CTE. We therefore checked whether this interaction was abolished in the absence of CTE by performing pull-down assays in a Δ*rhlE2*::3xFLAG-RhlE2$_{1-434}$ strain or co-expressing of T25-RhlE2$_{1-434}$ and T18-RNase E in bacterial two-hybrid assays. The pull-down assays showed that the interaction of RhlE2 with RNase E was lost in the absence of CTE (compare the level of RNase E on Coomassie gel in Figure 8A and in Figure 8B). The analysis of the eluates by mass-spectrometry still reveals the presence of some RNase E peptides (56 peptides in 3XFLAG-RhlE2$_{1-434}$ versus 74 peptides in 3XFLAG-RhlE2; Figure 8C). However, the bacterial two hybrid assay demonstrated unambiguously the involvement of the RhlE2 CTE in RNase E binding in vivo (Figure. 8D). We also cloned RhlE2 CTE into pKT25-based bacterial two-hybrid vector to assess interaction with pUT18-RNase E. A significant interaction was observed, suggesting RhlE2 CTE is involved in the interaction with RNase E (Supplementary Figure S13). Finally, we performed electrophoretic mobility shift assays using purified RhlE2 CTE (aa 434–639) and Cy-5 labelled shRNA^{8bp} and we could show that the CTE binds RNA and forms complex(es) with shRNA^{8bp} (Supplementary Figure S14). Having shown that RhlE2 CTE binds RNA and is needed to interact with RNase E, we also asked whether the CTE was required for RhlE2 catalytic activity. To address this question, the RhlE2$_{1-434}$ mutant was expressed in *E. coli* with an N-terminal His$_{10}$-Smt3-tag and purified as described previously (Figure 9A). The recombinant RhlE2$_{1-434}$ was still able to catalyze the release of ^{32}Pi from [γ-^{32}P] ATP in the presence of poly(U) RNA and the extent of ATP hydrolysis was proportional to enzyme concentration, with 56% of the ATP substrate was hydrolyzed in 15 minutes reaction at 100 ng/μl RhlE2$_{1-434}$ (Figure 9B). A specific activity of 0.011 nmol of ATP hydrolyzed per ng of protein in 15 min was calculated from the slope of the titration curve in the linear range (i.e. 696 mol of Pi formed per mol of protein and an estimated turnover of 46 min^{-1}), which is similar to the value observe for full-length RhlE2 (Figure 6B). The observed RNA-dependent phosphohydrolase activity can be attributed to RhlE2$_{1-434}$ insofar as the ATPase activity of the RhlE2$_{K51A,1-434}$ mutant in the presence poly(U) RNA was less than 1% of the activity of RhlE2$_{1-434}$ (Figure 9C). Next, we tested RhlE2$_{1-434}$ RNA preferences in respect to length and secondary structure (Figure 9D and E). Interestingly, we found RhlE2$_{1-434}$ ATPase activity with U41, U25, U16, U10 RNA substrate was 94, 59, 32, and 3% of the activity with poly(U) RNA, respectively (Figure 9D), as compared to the corresponding RhlE2 full-length ATPase activity that was 35, 12, 1 and <1%, respectively (Figure 6D). On the other hand, the RhlE2$_{1-434}$ ATPase activity was 1.5-fold and 2-fold higher with shRNA^{8bp} and RNA shRNA^{17bp} as compared to the single-stranded RNA ssRNA, while it was 3- and 4-fold higher with RhlE2 full length, respectively (Figures 6D and 9E). Finally, when RNA unwinding activity was assayed, the RhlE2$_{1-434}$ protein appeared less efficient, as a higher concentration of the truncated protein was required as compared to the full-length (Supplementary Figure S9C). From these results, we conclude that the CTE is dispensable for RhlE2 catalytic activity but affects RNA substrate recognition and RNA unwinding. Moreover, it is required for both its interaction with RNase E and overall, for RhlE2 to perform its regulatory functions *in vivo*.

RhlE2 affects the stability of some RNAs

Through its interaction with RNase E, RhlE2 could play a role in regulated RNA decay (69). In order to test this hypothesis, we assessed the half-life of some mRNAs in the wild type and Δ*rhlE2* mutant (Figure 10). For the analysis, we selected transcripts whose abundance appeared to be either down-regulated or up-regulated in our RNA-seq analysis (Figure 4). Up-regulated mRNAs in the *rhlE2* mutant, like PA1897, PA2314 or PA2268, displayed a 1.5- to 3-fold increase of their half-life compared to the wild type. On the other hand, the stability of *lasB*, a down-regulated mRNAs, does not seem to be affected by *rhlE2* deletion, which suggests that RhlE2 regulates it indirectly. In agreement with this hypothesis, we also observed a down-regulation of *lasB* expression in the Δ*rhlE2* mutant when we used a transcriptional *lasB–lacZ* fusion (70), reporting only on the activity of the *lasB* promoter rather than on the mRNA stability or translation rate (Supplementary Figure S15). These results suggest that RhlE2 could be an intrinsic part of the degradosome complex and affect the transcriptome of *P. aeruginosa* through its RNA remodelling activity.

DISCUSSION

This study was initially motivated by two observations based on a phylogenetic analysis of the RhlE group of proteobacterial RNA helicases. First, genes encoding RhlE proteins tend to expand in Proteobacteria through duplication or lateral gene transfer events, reaching up to six homologs in *Shewanella pealeana* ATCC 700345 (12). This suggests that this RNA helicase family is prone subfunctionalization via unknown mechanisms. Studying variations among RhlE homologs within the same organism would therefore open the door to a detailed understanding of correlative functional and mechanistic specialization in RNA helicases. Second, while the core of RhlE homologs both within and across bacteria is highly conserved, the C-terminal extensions are very diverse and evolve quickly. We therefore hypothesized that this part of the enzyme could be involved in significant mechanistic variations and sub-functionalization events. Unlike other organisms where RhlE proteins have been experimentally investigated, namely *E. coli*, *Y. pseudotuberculosis*, *M. tuberculosis*, *P. syringae* LZ4W (psychotropic strain) and *C. crescentus* (13–19), *P. aeruginosa* genome encodes two RhlE homologs; therefore, it represents an ideal model organism to investigate RhlE functional specialization and distinguish ancestral and newly emerging gene functions.

Cold adaptation is one of the most common functions connected to RNA helicases. It is linked to ability of RNA
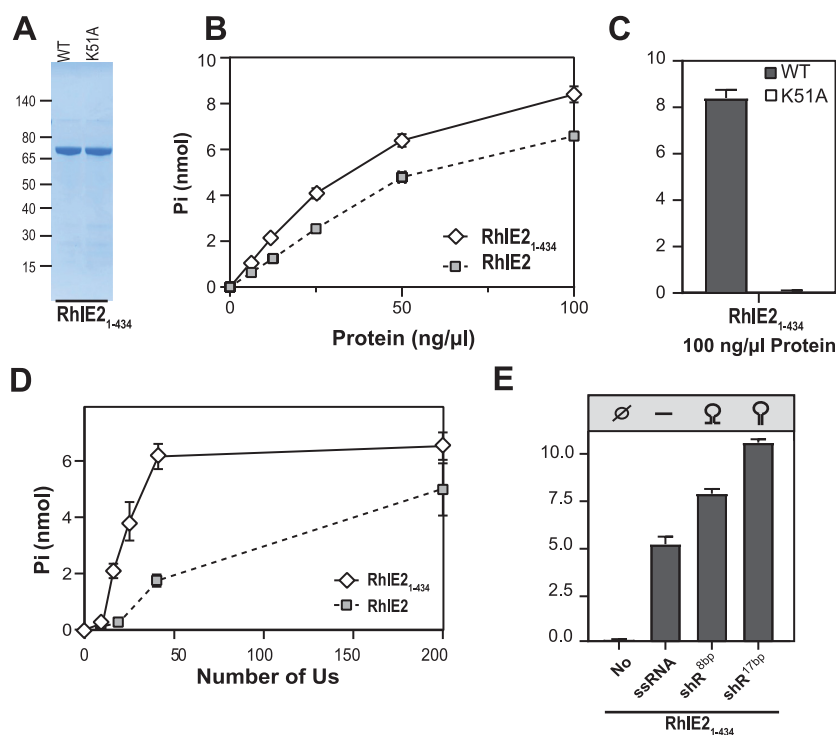
Figure 9. ATPase activity of recombinant RhlE2$_{1-434}$. (**A**) RhlE2$_{1-434}$ purification. Aliquots (2.5 µg) of the nickel-agarose preparations of RhlE2$_{1-434}$ (lane 1) and double mutant RhlE2$_{1-434, K51A}$ (lane 2) were analyzed by SDS-PAGE. The polypeptides were visualized by staining with Coomassie Blue dye. The positions and sizes (kDa) of marker polypeptides are indicated on the left. (**B**) ATPase. Reaction mixtures (15 µl) containing 50 mM Tris–HCl (pH 8.0), 1 mM DTT, 2 mM MgCl$_2$, 1 mM [γ-^{32}P] ATP, 250 ng/µl Poly(U), and 100 ng/µl of RhlE2$_{1-434}$ or RhlE2$_{1-434.K51A}$ mutant were incubated for 15 min at 37°C. The extends of ATP hydrolysis are plotted. (**C**) ATPase. Reaction mixtures (15 µl) containing 50 mM Tris–HCl (pH 8.0), 1 mM DTT, 2 mM MgCl$_2$, 1 mM [γ-^{32}P] ATP, 250 ng/µl Poly(U) and RhlE2(1–434) or K51 mutant protein as specified were incubated for 15 min at 37°C. Pi release was plotted as a function of input protein. (**D**) ATPase activity and RNA length. Reaction mixtures (15 µl) 50 mM Tris–HCl (pH 8.0), 5 mM DTT, 2 mM MgCl$_2$, 1 mM [γ-^{32}P] ATP, 2 µM polyribouridylic acid (either U41, U26, U16 or U10) as specified, and 50 ng/µl of RhlE2$_{1-434}$ were incubated for 15 min at 37°C. The extends of ATP hydrolysis are plotted. (**E**) RNA hairpin recognition. Reaction mixtures (15 µl) 50 mM Tris–HCl (pH 8.0), 5 mM DTT, 2 mM MgCl$_2$, 1 mM [γ-^{32}P] ATP, 2 µM of an oligoribonucleotide as specified and 50 ng/µl of RhlE2$_{1-434}$ were incubated for 15 min at 37°C. The extends of ATP hydrolysis are plotted. (B–E) Data are the average ± SEMs from three independent experiments.

helicases to resolve RNA secondary structures, which are stabilized at low temperatures, allowing the expression of gene(s) essential for growth on cold (11,15). Our phenotypic analysis of *P. aeruginosa rhlE1* and *rhlE2* mutants confirmed a role of both proteins in supporting cell growth at cold temperatures (16°C). Nonetheless, the two homologs are not redundant in their cold-resistance function since they cannot complement each other even when overexpressed. Moreover, beyond growth in the cold, deletion of *rhlE2* also affected cell motility, biofilm formation and production of virulence factors, ultimately resulting into a significant decrease in lethality in the *G. mellonella* infection model. At the molecular level, deletion of RhlE2 proved to affect 15% of the entire cellular transcripts in swarming conditions making it a global regulator. In agreement with our experimental observation, mining of publicly available data displaying the transcriptional profile of *P. aeruginosa* PA14 grown under 14 different environmental conditions (71) indicate that *rhlE2* expression levels are generally higher than *rhlE1*'s with overall little fluctuations upon environmental changes (Supplementary Figure S16).

Few other bacterial DEAD-box RNA helicases, namely CshA of *Listeria monocytogenes* and *Staphylococcus aureus* and RhpA of *Helicobacter pylori,* together with the HrpA

DExH-box helicase of *Borrelia burgdoferi*, have been shown to regulate expression of virulence traits (72–75). Another *P. aeruginosa* RNA helicase (PA2840, named DeaD) has been proposed as virulence regulator, due to its stimulatory effect on the synthesis of the type III secretion system regulator ExsA (30). Nonetheless, such significative impact on host-pathogen interactions in vivo as the one observed for RhlE2 has been rarely shown for RNA helicases. Phylogenetic analysis of RhlE proteins indicate that homologs closely related to RhlE2 are present in other bacteria, including environmental bacteria like *Azotobacter vinelandii* and several pathogens like *Klebsiella pneumoniae*, *Acinetobacter baumannii*, *Enterobacter clocae* and *Streptococcus dysgalactiae* subsp. *equisimilis* (Supplementary Figure S1), pointing at frequent horizontal gene transfer. Given these results, it may be worth investigating a possible role of RhlE2 as a virulence factor in other pathogenic species.

The phenotype of the mutants and the lack of cross-complementation between the two RhlE homologs indicate that the two proteins most likely act on different targets. Through in vitro characterization, we could link these functional differences to specific biochemical properties. In vitro, RhlE1 and RhlE2 possess an ATPase activity which is strictly RNA-dependent (Supplementary Figure S8) with-
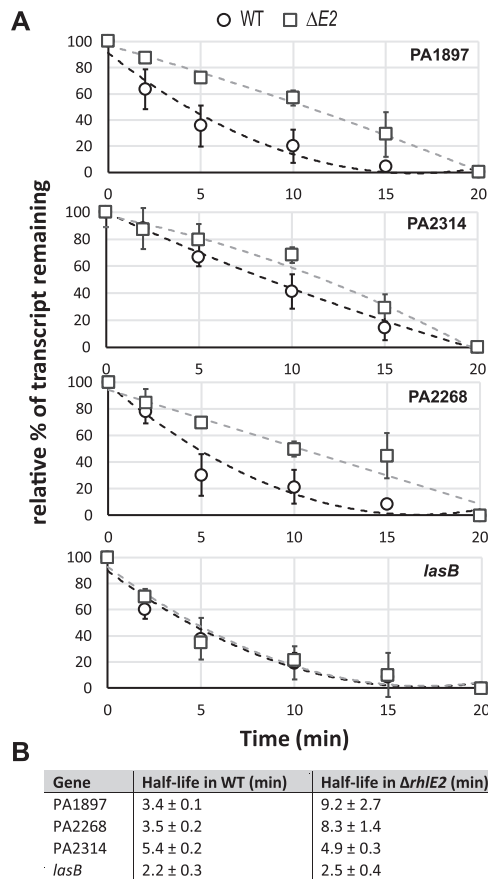
Figure 10. RhlE2 regulation of RNA stability. Determination of (**A**) the steady state levels and (**B**) half-life of PA1897, PA2314, PA2268 and *lasB* mRNA by RT-qPCR in the wild type PAO1 and Δ*rhlE2* mutant. Strains were grown in NYB medium until they reached an OD$_{600}$ of 1.5. Then 250 μg/ml rifampicin was added and samples after 1, 5, 10, 15 and 20 min were collected for RNA extraction and cDNA synthesis. The steady state levels of mRNAs were normalized to *rpoD* and *rplA* mRNA levels. The level of each mRNA levels at t_0 was set to 100% while at t_{20} was set to 0 and relative % of transcript remaining is plotted over time. The results represent the average of two independent experiments including each three technical replicates. The error bars in panel A represent standard deviation.

out any base specificity (see Figure 6E 41-mer ssRNA vs Figure 6D U41 RNA); this is expected since the RNA helicase catalytic core usually interacts with the 2′ OH ribose or the phosphate of the RNA backbone (76). By contrast, RhlE1 and RhlE2 display different RNA preferences, depending on RNA length and structure, and different RNA unwinding efficiencies. Unlike RhlE2, RhlE1 ATPase is activated by short RNA oligonucleotides (<16 nt), like it has been observed for the *E. coli* RhlE homolog (61). On the other hand, RhlE1 is not sensitive to the RNA structure, while RhlE2 prefers RNA molecules containing a hairpin (Figure 6E). Finally, RhlE2 seems more efficient than RhlE1 in unwinding RNA duplexes (Supplementary Figure S9). These data could be explained by a difference in the mechanism of interaction with RNA between RhlE1 and RhlE2. For example, the structure specificity may reflect a hairpin recognition domain within the C-terminal extension of RhlE2 that would stimulate the RNA helicase

core. In agreement, we found that the RhlE2 C-terminal extension binds RNA (Supplementary Figure S14). An in-depth RhlE2 biochemical and structural characterization is needed to explore how the protein can discriminate RNA secondary structure and subsequently tune its enzymatic activity.

The functional divergence between RhlE1 and RhlE2 could also be related to their different interacting partners within the cell. RNase E, the core endonuclease of the bacterial RNA degradosome, is co-eluted with FLAG-tagged RhlE2, but not with RhlE1. In agreement with our results, Van den Bossche and colleagues recently identified PA0428, under the name DeaD, as a possible component of the *P. aeruginosa* degradosome while studying the infectious interference of a bacteriophage protein with RNase E (77). We named here PA0428 RhlE2, while the DeaD/CsdA name should be attributed only to PA2840 to avoid any confusion.

Interaction of RhlE proteins with RNase E is a common theme: it has been observed in *E. coli*, *C. crescentus*, *P. syringae* LZ4W and *M. tuberculosis* (13,17,18,20). However, the way this interaction is brought about, and its physiological significance varies depending on the organism considered. Moreover, in *E. coli*, the RhlE interaction with RNase E has been observed only in vitro, where the protein can replace the RNA helicases RhlB and help with the degradation of structured RNA by PNPase (20); but the physiological conditions in which *E. coli* RhlE can replace RhlB are still unknown (78). A RhlB homolog is also present in *P. aeruginosa* and, interestingly, deletion of the encoding gene does not lead to the same phenotypes observed for *rhlE2* mutant (data not shown). Surprisingly, pre-treatment of *P. aeruginosa* cell extracts with RNase A before pull-down affects RhlE2 interaction with RNase E, suggesting that the interaction is mediated or stabilized by RNA. When the same experiment was performed in *C. crescentus*, the interaction resisted to the RNase A treatment indicating that interaction of RhlE with RNase E is a proper protein-protein interaction (13). The C-terminal extension of RhlE2 is necessary for the interaction since RNase E does not interact with RhlE2$_{1-434}$ construct in bacterial two-hybrid assays (Figure 8D). It is also required for RhlE2 to perform its regulatory function, since the RhlE2$_{1-434}$ protein does not restore in vivo the *rhlE2* mutant phenotypes to wild type levels. This suggests that RhlE2 mainly acts via the RNA degradosome. Indeed, we show that RhlE2 affects the half-life of some of the transcripts whose levels were affected by *rhlE2* deletion in the RNA-sequencing analysis. In *E. coli*, RNase E was shown to interact with RhlB by binding to the RecA2 domain and stimulating its ATPase activity (79,80). In *P. aeruginosa,* RNase E does not stimulate RhlE2 activity (data not shown), which probably reveals a different interaction of the two helicases with their endonuclease. Overall our work suggests that the composition and mode of action of the RNA degradosome might significantly differ between *P. aeruginosa* and *E. coli*, as suggested by the poor RNase E sequence conservation between these two species (81). We are currently investigating this question.

Finally, various RNA helicase inhibitors have been discovered in the past few years and are being investigated for their therapeutic potential (82,83). Given the urgent need for novel effective antimicrobials to combat *P. aeruginosa*

infections ([84](#)), a screening of small molecules inhibiting RhlE2 activity could lead to the identification of interesting drug candidates. Indeed, despite the structural similarities shared by all RNA helicases, protein-specific enzymatic properties and interaction particularities, like the ones distinguishing RhlE1 and RhlE2, could be used as a basis for the development of compounds targeting a given pathogen or cellular function with a high selectivity.

DATA AVAILABILITY

RNA-sequencing raw files and read counts per gene have been deposited in the NCBI Gene Expression Omnibus (GEO) database under the accession number GSE166986.

SUPPLEMENTARY DATA

Supplementary Data are available at NAR Online.

ACKNOWLEDGEMENTS

FUNDING

REFERENCES

1. Valentini,M. and Linder,P. (2021) Happy birthday: 30 years of RNA helicases. *Methods Mol. Biol.*, **2209**, 17–34.
2. Linder,P., Lasko,P.F., Ashburner,M., Leroy,P., Nielsen,P.J., Nishi,K., Schnier,J. and Slonimski,P.P. (1989) Birth of the D-E-A-D box. *Nature*, **337**, 121–122.
3. Gorbalenya,A.E. and Koonin,E.V. (1993) Helicases: amino acid sequence comparisons and structure-function relationships. *Curr. Opin. Struct. Biol.*, **3**, 419–429.
4. Linder,P. and Daugeron,M.C. (2000) Are DEAD-box proteins becoming respectable helicases? *Nat. Struct. Biol.*, **7**, 97–99.
5. Fiorini,F., Boudvillain,M. and Le Hir,H. (2012) Tight intramolecular regulation of the human Upf1 helicase by its N- and C-terminal domains. *Nucleic Acids Res.*, **41**, 2404–2415.
6. Pietras,Z., Hardwick,S.W., Swiezewski,S. and Luisi,B.F. (2013) Potential regulatory interactions of *Escherichia coli* RraA protein with DEAD-box helicases. *J. Biol. Chem.*, **288**, 31919–31929.
7. Kossen,K., Karginov,F.V. and Uhlenbeck,O.C. (2002) The carboxy-terminal domain of the DExDH protein YxiN is sufficient to confer specificity for 23S rRNA. *J. Mol. Biol.*, **324**, 625–636.
8. Diges,C.M. and Uhlenbeck,O.C. (2001) *Escherichia coli* DbpA is an RNA helicase that requires hairpin 92 of 23S rRNA. *EMBO J.*, **20**, 5503–5512.
9. Redder,P., Hausmann,S., Khemici,V., Yasrebi,H. and Linder,P. (2015) Bacterial versatility requires DEAD-box RNA helicases. *FEMS Microbiol. Rev.*, **39**, 392–412.
10. Kaberdin,V.R. and Bläsi,U. (2013) Bacterial helicases in post-transcriptional control. *Biochim. Biophys. Acta*, **1829**, 878–883.
11. Owttrim,G.W. (2013) RNA helicases: diverse roles in prokaryotic response to abiotic stress. *RNA Biol*, **10**, 96–110.
12. Lopez-Ramirez,V., Alcaraz,L.D., Moreno-Hagelsieb,G. and Olmedo-Alvarez,G. (2011) Phylogenetic distribution and evolutionary history of bacterial DEAD-Box proteins. *J. Mol. Evol.*, **72**, 413–431.
13. Aguirre,A.A., Vicente,A.M., Hardwick,S.W., Alvelos,D.M., Mazzon,R.R., Luisi,B.F. and Marques,M.V. (2017) Association of the cold shock DEAD-Box RNA helicase RhlE to the RNA degradosome in *Caulobacter crescentus*. *J. Bacteriol.*, **199**, e00135-17.
14. Virtanen,J.P., Keto-Timonen,R., Jaakkola,K., Salin,N. and Korkeala,H. (2018) Changes in transcriptome of *Yersinia pseudotuberculosis* IP32953 grown at 3 and 28°C detected by RNA sequencing shed light on cold adaptation. *Front Cell Infect Microbiol*, **8**, 2235–2988.
15. Awano,N., Xu,C., Ke,H., Inoue,K., Inouye,M. and Phadtare,S. (2007) Complementation analysis of the cold-sensitive phenotype of the *Escherichia coli* csdA deletion strain. *J. Bacteriol.*, **189**, 5808–5815.
16. Ohmori,H. (1994) Structural analysis of the *rhlE* gene of *Escherichia coli*. *Idengaku zasshi*, **69**, 1–12.
17. Płociński,P., Macios,M., Houghton,J., Niemiec,E., Płocińska,R., Brzostek,A., Słomka,M., Dziadek,J., Young,D. and Dziembowski,A. (2019) Proteomic and transcriptomic experiments reveal an essential role of RNA degradosome complexes in shaping the transcriptome of *Mycobacterium tuberculosis*. *Nucleic Acids Res.*, **47**, 5892–5905.
18. Purusharth,R.I., Klein,F., Sulthana,S., Jäger,S., Jagannadham,M.V., Evgenieva-Hackenberg,E., Ray,M.K. and Klug,G. (2005) Exoribonuclease R interacts with endoribonuclease E and an RNA helicase in the psychrotrophic bacterium *Pseudomonas syringae* Lz4W. *J. Biol. Chem.*, **280**, 14572–14578.
19. Jain,C. (2008) The *E. coli* RhlE RNA helicase regulates the function of related RNA helicases during ribosome assembly. *RNA*, **14**, 381–389.
20. Khemici,V., Toesca,I., Poljak,L., Vanzo,N.F. and Carpousis,A.J. (2004) The RNase E of *Escherichia coli* has at least two binding sites for DEAD-box RNA helicases: functional replacement of RhlB by RhlE. *Mol. Microbiol.*, **54**, 1422–1430.
21. Green,S.K., Schroth,M.N., Cho,J.J., Kominos,S.K. and Vitanza-jack,V.B. (1974) Agricultural plants and soil as a reservoir for *Pseudomonas aeruginosa*. *Appl. Microbiol.*, **28**, 987–991.
22. Hardalo,C. and Edberg,S.C. (1997) *Pseudomonas aeruginosa*: assessment of risk from drinking water. *Crit. Rev. Microbiol.*, **23**, 47–75.
23. Palleroni,N.J. (2015) Pseudomonas. *Bergey's Manual of Systematics of Archaea and Bacteria*, https://doi.org/10.1002/9781118960608.gbm01210.
24. Garcia-Clemente,M., de la Rosa,D., Máiz,L., Girón,R., Blanco,M., Olveira,C., Canton,R. and Martinez-García,M.A. (2020) Impact of *Pseudomonas aeruginosa* Infection on Patients with Chronic Inflammatory Airway Diseases. *J. Clin. Med.*, **9**, 3800.
25. Urwin,L., Okurowska,K., Crowther,G., Roy,S., Garg,P., Karunakaran,E., MacNeil,S., Partridge,L.J., Green,L.R. and Monk,P.N. (2020) Corneal Infection Models: Tools to Investigate the Role of Biofilms in Bacterial Keratitis. *Cells*, **9**, 2450.
26. Costerton,J.W., Stewart,P.S. and Greenberg,E.P. (1999) Bacterial biofilms: a common cause of persistent infections. *Science*, **284**, 1318–1322.
27. De Oliveira,D.M.P., Forde,B.M., Kidd,T.J., Harris,P.N.A., Schembri,M.A., Beatson,S.A., Paterson,D.L. and Walker,M.J. (2020) Antimicrobial resistance in ESKAPE pathogens. *Clin. Microbiol. Rev.*, **33**, e00181-19.
28. Pendleton,J.N., Gorman,S.P. and Gilmore,B.F. (2013) Clinical relevance of the ESKAPE pathogens. *Expert Rev. Anti Infect. Ther.*, **11**, 297–308.
29. Lyczak,J.B., Cannon,C.L. and Pier,G.B. (2000) Establishment of *Pseudomonas aeruginosa* infection: lessons from a versatile opportunist. *Microbes Infect.*, **2**, 1051–1060.
30. Intile,P.J., Balzer,G.J., Wolfgang,M.C. and Yahr,T.L. (2015) The RNA helicase DeaD stimulates ExsA translation to promote

expression of the *Pseudomonas aeruginosa* type III secretion system. *J. Bacteriol.*, **197**, 2664–2674.

31. Sezonov,G., Joseleau-Petit,D. and D'Ari,R. (2007) *Escherichia coli* physiology in Luria-Bertani broth. *J. Bacteriol.*, **189**, 8746–8749.

32. Miller,J.H. (1972) In: *Experiments in Molecular Genetics*. Cold Spring Harbor Laboratory, NY.

33. Sambrook,J., Fritsch,E.F. and Maniatis,T. (1989) In: *Molecular Cloning: A Laboratory Manual*. 2nd edn. Cold Spring Harbor Laboratory Press, NY.

34. Pessi,G. and Haas,D. (2000) Transcriptional control of the hydrogen cyanide biosynthetic genes *hcnABC* by the anaerobic regulator ANR and the quorum-sensing regulators LasR and RhlR in *Pseudomonas aeruginosa*. *J. Bacteriol.*, **182**, 6940–6949.

35. Bolger,A.M., Lohse,M. and Usadel,B. (2014) Trimmomatic: a flexible trimmer for Illumina sequence data. *Bioinformatics*, **30**, 2114–2120.

36. Langmead,B. and Salzberg,S.L. (2012) Fast gapped-read alignment with Bowtie 2. *Nat. Methods*, **9**, 357–359.

37. Anders,S., Pyl,P.T. and Huber,W. (2015) HTSeq–a Python framework to work with high-throughput sequencing data. *Bioinformatics*, **31**, 166–169.

38. RCoreTeam (2020) In: *R: A Language and Environment for Statistical Computing*. R Foundation for Statistical Computing, Vienna, Austria.

39. Robinson,M.D., McCarthy,D.J. and Smyth,G.K. (2010) edgeR: a Bioconductor package for differential expression analysis of digital gene expression data. *Bioinformatics*, **26**, 139–140.

40. Ritchie,M.E., Phipson,B., Wu,D., Hu,Y., Law,C.W., Shi,W. and Smyth,G.K. (2015) limma powers differential expression analyses for RNA-sequencing and microarray studies. *Nucleic Acids Res.*, **43**, e47.

41. Pruitt,K.D., Brown,G.R., Hiatt,S.M., Thibaud-Nissen,F., Astashyn,A., Ermolaeva,O., Farrell,C.M., Hart,J., Landrum,M.J., McGarvey,K.M. *et al.* (2014) RefSeq: an update on mammalian reference sequences. *Nucleic Acids Res.*, **42**, D756–D763.

42. Edgar,R.C. (2004) MUSCLE: multiple sequence alignment with high accuracy and high throughput. *Nucleic Acids Res.*, **32**, 1792–1797.

43. Li,W. and Godzik,A. (2006) Cd-hit: a fast program for clustering and comparing large sets of protein or nucleotide sequences. *Bioinformatics*, **22**, 1658–1659.

44. Price,M.N., Dehal,P.S. and Arkin,A.P. (2010) FastTree 2 – approximately maximum-likelihood trees for large alignments. *PLoS One*, **5**, e9490.

45. Stöver,B.C. and Müller,K.F. (2010) TreeGraph 2: combining and visualizing evidence from different phylogenetic analyses. *BMC Bioinformatics*, **11**, 7.

46. Kearns,D.B. (2010) A field guide to bacterial swarming motility. *Nat. Rev. Microbiol.*, **8**, 634–644.

47. Tremblay,J. and Déziel,E. (2010) Gene expression in *Pseudomonas aeruginosa* swarming motility. *BMC Genomics*, **11**, 587.

48. Overhage,J., Bains M Fau - Brazas,M.D., Brazas Md Fau - Hancock,R.E.W. and Hancock,R.E. (2008) Swarming of *Pseudomonas aeruginosa* is a complex adaptation leading to increased production of virulence factors and antibiotic resistance. *J. Bacteriol.*, **190**, 2671–2679.

49. Merritt,J.H., Ha,D.G., Cowles,K.N., Lu,W., Morales,D.K., Rabinowitz,J., Gitai,Z. and O'Toole,G.A. (2010) Specific control of *Pseudomonas aeruginosa* surface-associated behaviors by two c-di-GMP diguanylate cyclases. *mBio*, **1**, e00183-10.

50. Watanabe,S., Morimoto,D., Fukumori,F., Shinomiya,H., Nishiwaki,H., Kawano-Kawada,M., Sasai,Y., Tozawa,Y. and Watanabe,Y. (2012) Identification and characterization of D-hydroxyproline dehydrogenase and Delta1-pyrroline-4-hydroxy-2-carboxylate deaminase involved in novel L-hydroxyproline metabolism of bacteria: metabolic convergent evolution. *J. Biol. Chem.*, **287**, 32674–32688.

51. McIver,K.S., Kessler,E., Olson,J.C. and Ohman,D.E. (1995) The elastase propeptide functions as an intramolecular chaperone required for elastase activity and secretion in *Pseudomonas aeruginosa*. *Mol. Microbiol.*, **18**, 877–889.

52. McMorran,B.J., Kumara,H., Sullivan,K. and Lamont,I.L. (2001) Involvement of a transformylase enzyme in siderophore synthesis in *Pseudomonas aeruginosa*. *Microbiology*, **147**, 1517–1524.

53. Déziel,E., Lépine,F., Milot,S. and Villemur,R. (2003) *rhlA* is required for the production of a novel biosurfactant promoting swarming motility in *Pseudomonas aeruginosa*:

54. 3-(3-hydroxyalkanoyloxy)alkanoic acids (HAAs), the precursors of rhamnolipids. *Microbiology*, **149**, 2005–2013.

54. Passador,L., Cook,J.M., Gambello,M.J., Rust,L. and Iglewski,B.H. (1993) Expression of *Pseudomonas aeruginosa* virulence genes requires cell-to-cell communication. *Science*, **260**, 1127–1130.

55. Brint,J.M. and Ohman,D.E. (1995) Synthesis of multiple exoproducts in *Pseudomonas aeruginosa* is under the control of RhlR-RhlI, another set of regulators in strain PAO1 with homology to the autoinducer-responsive LuxR-LuxI family. *J. Bacteriol.*, **177**, 7155–7163.

56. Morihara,K. (1995) In: *Methods in Enzymology*. Academic Press, Vol. **248**, pp. 242–253.

57. Lau,G.W., Hassett,D.J., Ran,H. and Kong,F. (2004) The role of pyocyanin in *Pseudomonas aeruginosa* infection. *Trends Mol. Med.*, **10**, 599–606.

58. Junqueira,J.C. (2012) *Galleria mellonella* as a model host for human pathogens. *Virulence*, **3**, 474–476.

59. Putnam,A.A. and Jankowsky,E. (2013) DEAD-box helicases as integrators of RNA, nucleotide and protein binding. *Biochim. Biophys. Acta*, **1829**, 884–893.

60. Jankowsky,E. (2011) RNA helicases at work: binding and rearranging. *Trends Biochem. Sci.*, **36**, 19–29.

61. Bizebard,T., Ferlenghi,I., Iost,I. and Dreyfus,M. (2004) Studies on three *E. coli* DEAD-box helicases point to an unwinding mechanism different from that of model DNA helicases. *Biochemistry*, **43**, 7857–7866.

62. Mallam,A.L., Sidote,D.J. and Lambowitz,A.M. (2014) Molecular insights into RNA and DNA helicase evolution from the determinants of specificity for a DEAD-box RNA helicase. *eLife*, **3**, e04630.

63. Tauchert,M.J., Fourmann,J.B., Luhrmann,R. and Ficner,R. (2017) Structural insights into the mechanism of the DEAH-box RNA helicase Prp43. *eLife*, **6**, e21510.

64. Boneberg,F.M., Brandmann,T., Kobel,L., van den Heuvel,J., Bargsten,K., Bammert,L., Kutay,U. and Jinek,M. (2019) Molecular mechanism of the RNA helicase DHX37 and its activation by UTP14A in ribosome biogenesis. *RNA*, **25**, 685–701.

65. Sengoku,T., Nureki,O., Nakamura,A., Kobayashi,S. and Yokoyama,S. (2006) Structural basis for RNA unwinding by the DEAD-box protein Drosophila Vasa. *Cell*, **125**, 287–300.

66. Karimova,G., Pidoux,J., Ullmann,A. and Ladant,D. (1998) A bacterial two-hybrid system based on a reconstituted signal transduction pathway. *PNAS*, **95**, 5752.

67. Xu,L., Wang,L., Peng,J., Li,F., Wu,L., Zhang,B., Lv,M., Zhang,J., Gong,Q., Zhang,R. *et al.* (2017) Insights into the structure of dimeric RNA helicase CsdA and indispensable role of its C-terminal regions. *Structure*, **25**, 1795–1808.

68. Giraud,C., Hausmann,S., Lemeille,S., Prados,J., Redder,P. and Linder,P. (2015) The C-terminal region of the RNA helicase CshA is required for the interaction with the degradosome and turnover of bulk RNA in the opportunistic pathogen *Staphylococcus aureus*. *RNA Biol*, **12**, 658–674.

69. Apirion,D. (1978) Isolation, genetic mapping and some characterization of a mutation in *Escherichia coli* that affects the processing of ribonucleic acid. *Genetics*, **90**, 659–671.

70. Preston,M.J., Seed,P.C., Toder,D.S., Iglewski,B.H., Ohman,D.E., Gustin,J.K., Goldberg,J.B. and Pier,G.B. (1997) Contribution of proteases and LasR to the virulence of *Pseudomonas aeruginosa* during corneal infections. *Infect. Immun.*, **65**, 3086–3090.

71. Dötsch,A., Schniederjans,M., Khaledi,A., Hornischer,K., Schulz,S., Bielecka,A., Eckweiler,D., Pohl,S. and Häussler,S. (2015) The *Pseudomonas aeruginosa* transcriptional landscape is shaped by environmental heterogeneity and genetic variation. *mBio*, **6**, e00749-15.

72. El Mortaji,L., Aubert,S., Galtier,E., Schmitt,C., Anger,K., Redko,Y., Quentin,Y. and De Reuse,H. (2018) The sole DEAD-Box RNA helicase of the gastric pathogen *Helicobacter pylori* is essential for colonization. *mBio*, **9**, e02071-17.

73. Netterling,S., Bäreclev,C., Vaitkevicius,K. and Johansson,J. (2016) RNA helicase important for *Listeria monocytogenes* hemolytic activity and virulence factor expression. *Infect. Immun.*, **84**, 67.

74. Oun,S., Redder,P., Didier,J.P., François,P., Corvaglia,A.R., Buttazzoni,E., Giraud,C., Girard,M., Schrenzel,J. and Linder,P.

(2013) The CshA DEAD-box RNA helicase is important for quorum sensing control in *Staphylococcus aureus*. *RNA Biol*, **10**, 157–165.

75. Salman-Dilgimen,A., Hardy,P.O., Dresser,A.R. and Chaconas,G. (2011) HrpA, a DEAH-box RNA helicase, is involved in global gene regulation in the Lyme disease spirochete. *PLoS One*, **6**, e22168.

76. Ozgur,S., Buchwald,G., Falk,S., Chakrabarti,S., Prabu,J.R. and Conti,E. (2015) The conformational plasticity of eukaryotic RNA-dependent ATPases. *FEBS J.*, **282**, 850–863.

77. Van den Bossche,A., Hardwick,S.W., Ceyssens,P.J., Hendrix,H., Voet,M., Dendooven,T., Bandyra,K.J., De Maeyer,M., Aertsen,A., Noben,J.P. *et al.* (2016) Structural elucidation of a novel mechanism for the bacteriophage-based inhibition of the RNA degradosome. *eLife*, **5**, e16413.

78. Khemici,V., Poljak,L., Toesca,I. and Carpousis,A.J. (2005) Evidence in vivo that the DEAD-box RNA helicase RhlB facilitates the degradation of ribosome-free mRNA by RNase E. *PNAS*, **102**, 6913–6918.

79. Chandran,V., Poljak,L., Vanzo,N.F., Leroy,A., Miguel,R.N., Fernandez-Recio,J., Parkinson,J., Burns,C., Carpousis,A.J. and Luisi,B.F. (2007) Recognition and cooperation between the ATP-dependent RNA helicase RhlB and ribonuclease RNase E. *J. Mol. Biol.*, **367**, 113–132.

80. Bruce,H.A., Du,D., Matak-Vinkovic,D., Bandyra,K.J., Broadhurst,R.W., Martin,E., Sobott,F., Shkumatov,A.V. and Luisi,B.F. (2018) Analysis of the natively unstructured

RNA/protein-recognition core in the *Escherichia coli* RNA degradosome and its interactions with regulatory RNA/Hfq complexes. *Nucleic Acids Res.*, **46**, 387–402.

81. Aït-Bara,S., Carpousis,A.J. and Quentin,Y. (2015) RNase E in the γ-proteobacteria: conservation of intrinsically disordered noncatalytic region and molecular evolution of microdomains. *Mol. Genet. Genomics*, **290**, 847–862.

82. Shadrick,W.R., Ndjomou,J., Kolli,R., Mukherjee,S., Hanson,A.M. and Frick,D.N. (2013) Discovering new medicines targeting helicases: challenges and recent progress. *J. Biomol. Screen*, **18**, 761–781.

83. Abdelkrim,Y.Z., Banroques,J. and Kyle Tanner,N. (2021) Known inhibitors of RNA helicases and their therapeutic potential. *Methods Mol. Biol.*, **2209**, 35–52.

84. Tacconelli,E., Carrara,E., Savoldi,A., Harbarth,S., Mendelson,M., Monnet,D.L., Pulcini,C., Kahlmeter,G., Kluytmans,J., Carmeli,Y. *et al.* (2018) WHO Pathogens Priority List Working Group. Discovery, research, and development of new antibiotics: the WHO priority list of antibiotic-resistant bacteria and tuberculosis. *Lancet Infect Dis.*, **18**, 318–327.

85. Guzman,L.M., Belin,D., Carson,M.J. and Beckwith,J. (1995) Tight regulation, modulation, and high-level expression by vectors containing the arabinose PBAD promoter. *J. Bacteriol.*, **177**, 4121–4130.